arXiv:1002.1473v1 [nucl-th] 7 Feb 2010

Free magnetized knots of parity-violating deconfined matter in heavy-ion collisions

M. N. Chernodub*

Laboratoire de Mathématiques et Physique Théorique, Université François-Rabelais Tours,
Fédération Denis Poisson - CNRS, Parc de Grandmont, 37200 Tours, France
DMPA, University of Gent, Krijgslaan 281, S9, B-9000 Gent, Belgium

(Dated: February 7, 2010)

We show that the local parity violation in the quark-gluon plasma supports existence of free (meta)stable knots of deconfined hot quark matter stabilized by superstrong magnetic fields. The magnetic field in the knots resembles the spheromak plasma state of the magnetic confinement approach to nuclear fusion. The size of the knot is quantized, being inversely proportional to the chiral conductivity of the quark-gluon plasma. The parity symmetry is broken inside the knot. Particles produced in the decays of the knots have unusual azimuthal distribution and specific flavor content. We argue that these knots may be created in noncentral heavy-ion collisions.

PACS numbers: 25.75.-q,25.75.Nq,11.30.Er

MOTIVATION

Heavy-ion collisions may generate very strong magnetic fields with the magnitude of the order of the QCD scale. The lowest bound of the maximal strength of the magnetic field B that can emerge in noncentral collisions of Pb–Pb ions at the Large Hadron Collider (LHC) at CERN was estimated in [1] to be

$$e B^{\max}_{\mathrm{LHC}} \gtrsim 15\, m_\pi^2\,, \qquad (1)$$

where $e = |e|$ is the absolute value of the electron charge and $m_\pi \approx 140\,\mathrm{MeV}$ is the pion mass. This superstrong long-ranged magnetic field acts as an external field on electrically charged quarks and antiquarks that constitute the hot and dense quark-gluon matter created in the collision.

Theoretically, the magnetic field of the strength (1) may lead to various nonperturbative effects such that (i) a modification of the phase diagram of QCD via inequivalent shifts of both the chiral [2] and deconfining finite-temperature transitions [3]; (ii) an enhancement of the chiral condensate [4] via an enforcement of the dynamical chiral symmetry breaking [5]; (iii) an anomaly-mediated creation of a stack of parallel domain walls made of neutral pions in a dense plasma [6]; etc.

Strikingly, the superstrong hadron-scale magnetic field has already exposed itself experimentally. Recently, the STAR collaboration has found possible signatures of parity violation in locally macroscopic domains of hot, strongly interacting matter created in heavy-ion collisions at the RHIC experimental facility [7]. Such domains may arise due to a nonvanishing expectation value of the gluon topological charge that breaks both parity (P) and charge-parity (CP) symmetries. In the hot quark-gluon plasma the spontaneous generation of the parity-violating domains – suggested theoretically in Ref. [8] – may be revealed with the help of a very strong magnetic field which is created in a noncentral heavy-ion collision as well. The key point is that in the parity-violating background the external magnetic field leads to generation of an electric current. This unusual phenomenon – used in the experiment [7] to reveal the local parity violations via electric charge fluctuations – is now known as the Chiral Magnetic Effect (CME) [9, 10]. There exist also a numerical evidence of existence of the CME based on the lattice simulations of QCD [11].

The essence of the CME may be formulated in the following way: if a magnetic field $\vec B$ is applied to a system characterized by an asymmetry between the number of right- and left-handed fermions (quarks), then an electric current $\vec j$ is induced along the magnetic field axis [10]:

$$\vec j = \sigma_\chi \vec B\,. \qquad (2)$$

The external electric field is assumed to be absent, $\vec E = 0$.

In (2) the quantity σ_χ is the chiral conductivity [10] and

$$j_\mu = \sum_f e_f \bar\psi_f \gamma_\mu \psi_f\,, \qquad (3)$$

is the conserved electromagnetic four-current of the quarks. The vector $\vec j$ represents the spatial components of (3). In Eq. (3) e_q and ψ_f are the electric charge and the field of the f^{th} quark flavor, respectively, and γ_μ is the Dirac matrix. The left-right quark asymmetry in the quark-gluon plasma – that is needed for a realization of the CME (2) – may be induced by various parity-odd (topological) effects [10].

The parity-odd law (2) can be contrasted with the ordinary Ohm's law, $\vec j = \sigma \vec E$, which is certainly a parity-even feature of the system. Here σ is the conventional conductivity, and the external magnetic field is assumed to be absent, $\vec B = 0$.

We show that the presence of the chiral conductivity (2) – induced by topological QCD effects – may lead to existence of (meta)stable knots made of the magnetic field that is frozen in the hot quark-gluon plasma in a magnetohydrodynamic equilibrium. In general, knotted configurations are of wide interest in many areas of physics. One can encounter them in particle physics [12], fluid dynamics [13], plasma physics [14], condensed matter physics [15], and classical field theory [16, 17]. Knotted light solutions to the vacuum Maxwell equations are known theoretically [18], and very recently they were discovered experimentally in laser beams in a complementary approach of Ref. [19]. Here we show that free knotted objets can be created in heavy-ion collisions as well.

KNOT SOLUTIONS IN PARITY-ODD PLASMA

The classical Maxwell equations of motion are

$$\partial_\mu F^{\mu\nu} = j^\nu\,, \qquad \partial_\mu \widetilde{F}^{\mu\nu} = 0\,, \tag{4}$$

where $F^{\mu\nu}$ is the electromagnetic field strength tensor, $\widetilde{F}^{\mu\nu} = (1/2)\varepsilon^{\mu\nu\alpha\beta} F_{\alpha\beta}$ is its dual, and j_μ is the electric current density (3). It is convenient to rewrite Eqs. (4) in terms of electric $\vec{E}$ and magnetic $\vec{B}$ fields:

$$\vec{\nabla} \times \vec{B} - \frac{\partial \vec{E}}{\partial t} = \vec{j}\,, \tag{5}$$

$$\vec{\nabla} \cdot \vec{E} = \rho\,, \tag{6}$$

$$\vec{\nabla} \times \vec{E} + \frac{\partial \vec{B}}{\partial t} = 0\,, \tag{7}$$

$$\vec{\nabla} \cdot \vec{B} = 0\,, \tag{8}$$

where $\rho = j_0$ is the electric charge density.

We are interested in static electrically neutral solutions, and therefore we set

$$\vec{E} = 0\,, \qquad \rho = 0\,, \qquad \frac{\partial \vec{B}}{\partial t} = 0\,. \tag{9}$$

The quark-gluon plasma is conducting, and therefore the Maxwell equations should be supplemented with the laws, that account for effects of the medium on the propagation of the electric current. In the absence of the bulk electric field (9) this transport property is determined by the CME, Eq. (2).

The requirement (9) is automatically consistent with Eqs. (6) and (7), while Eqs. (5) and (8) give us a simpler system of equations:

$$\vec{\nabla} \times \vec{B} = \sigma_\chi \vec{B}\,, \tag{10}$$

$$\vec{\nabla} \cdot \vec{B} = 0\,. \tag{11}$$

We are looking for solutions of Eqs. (10) and (11) inside a ball of a certain radius R. As we discuss below, the quark matter inside the ball, $r < R$ should be in a deconfined phase while the state outside the ball corresponds to the confinement phase. Therefore, the electric current $\vec{j}$ in a stable configuration must always be tangent to the boundary of the ball, $\vec{j} \cdot \hat{r} = 0$. Here the unit vector in the r direction, $\hat{r}$, represents the outward-normal vector to the boundary of the ball. Then Eq. (2) gives us the following boundary condition:

$$\hat{r} \cdot \vec{B}(\vec{r})\Big|_{r=R} = 0\,. \tag{12}$$

The system of equations (10) and (11) is very well known because it plays an important role in usual plasma physics. The corresponding solutions are usually called Chandrasekhar-Kendall states following the authors who stressed importance of these solutions for astrophysical plasmas [20]. In the theory of nuclear fusion plasmas, the eigenvectors of (10) and (11) are known as Taylor states [22]. Such states are ultimate minimum-energy configurations in the plasma equilibrium.

Mathematically, Eqs. (10), (11) and (12) define an eigensystem of the curl operator "$\vec{\nabla}\times$". Usually, an eigenvalue problem is formulated in a fixed domain of space, so that the unknowns are eigenvalues. In our case the eigenvalue in Eq. (10) is fixed by the known chiral conductivity σ_χ, which is assumed, for the sake of simplicity, to be coordinate-independent. The unknown quantity is the radius of the ball, which enters the system of equations via the boundary condition (12).

In the spherical domain the curl operator has a discrete set of quantized eigenvalues and eigenvectors, that were described in details in Refs. [20, 21, 23]. Adopting these results to our notations, we find that Eqs. (10), (11), (12) have solutions in spherical balls of the quantized radii,

$$R^{(l)}_k = \frac{\kappa^{(l)}_k}{\sigma_\chi}\,, \qquad l, k = 1, 2, 3, \dots\,, \tag{13}$$

where $\kappa^{(l)}_k$ is the kth positive zero of the Bessel function $J_{n+1/2}(\kappa)$. In our paper we are interested in the knot solution with the smallest possible radius

$$R_0 = \frac{\kappa_0}{\sigma_\chi}\,, \qquad \kappa_0 \equiv \kappa^{(1)}_1 = 4.49341\dots\,. \tag{14}$$

In the spherical coordinates the corresponding magnetic field configuration is

$$\vec{B}(r,\theta,\varphi) = B_0 \big[u(\sigma_\chi r, \theta)\, \hat{r} + v(\sigma_\chi r, \theta)\, \hat{\theta} + w(\sigma_\chi r, \theta)\, \hat{\varphi} \big]\,, \tag{15}$$

for $r \leqslant R_0$, and $\vec{B}(r,\theta,\varphi) = 0$ for $r > R_0$. In Eq. (15)

$$u(\xi,\theta) = \frac{2}{\xi^3} \left(\sin\xi - \xi\, \cos\xi \right) \cos\theta\,, \tag{16}$$

$$v(\xi,\theta) = \frac{1}{\xi^3} \left(\sin\xi - \xi\, \cos\xi - \xi^2\, \sin\xi \right) \sin\theta\,, \tag{17}$$

$$w(\xi,\theta) = \frac{1}{\xi^2} \left(\sin\xi - \xi\, \cos\xi \right) \sin\theta\,, \tag{18}$$

and $\hat{\theta}$ and $\hat{\varphi}$ are the unit vectors in the azimuthal and polar directions, respectively. The azimuthal angle, $\theta \in (0, \pi)$ is inclination from the z axis, while the polar angle, $\varphi \in (-\pi, \pi)$, operates in the xy plane. The coordinate-independent factor B_0 in Eq. (15) is a free parameter.

The structure of the magnetic field of the solution (15)–(18) is rather complicated. The solution consist of an infinite number of nested (deformed) tori, and the degree of the deformation varies with the torus size. The magnetic field lines wrap around each torus and produce multiple self-linkages, what is a typical feature of all Chandrasekhar-Kendall states [18]. Therefore we call the solution (15)–(18) as "knot". The structure of typical magnetic lines and electric currents in the knot is illustrated in Fig. 1.

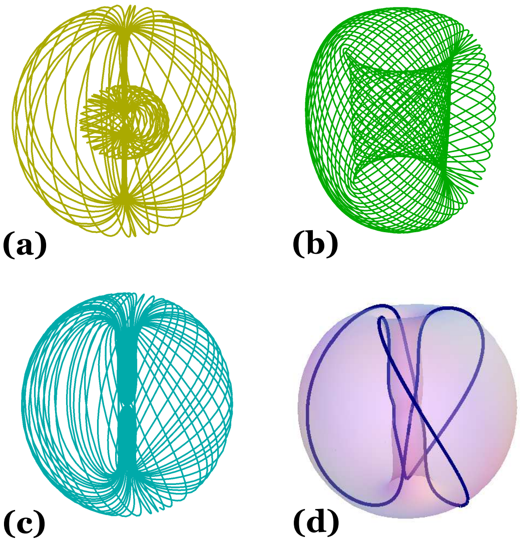

FIG. 1. Typical structures formed by the lines of the magnetic field and, equivalently, by the electric currents. The lines wind around different nested tori inside the same knot solution (15)–(18). The figures are described in the text.

It is convenient to label each structure by specifying the maximal size $r_{\max}$ of the (deformed) torus in units of the overall knot size R_0, Eq. (14). In the largest structures the field wind around two tori simultaneously [Fig. 1(a), $r_{\max}/R_0 = 0.96$]. As the size becomes smaller, the structure of the magnetic fields gets a conventional torus shape [Fig. 1(b), $r_{\max}/R_0 = 0.91$]. Yet another torus shape can be found at lower radii [Fig. 1(c), $r_{\max}/R_0 = 0.77$]. At particular radii the magnetic field lines form well-known knotted structures. For example, at $r_{\max}/R_0 = 0.88566$, the magnetic lines are trefoil knots, which wrap around a torus, Fig. 1(d).

Notice, that despite the knot occupies an ideally spherical region, its interior is only axially (not spherically) symmetric. Moreover, the knot is a parity-odd object: its reflected image cannot be superimposed on itself. A mirror image of a left-handed knot is a right-handed knot.

In an astrophysical applications the knot (15)-(18) was used to model magnetic field patterns of the Crab Nebula [24]. At much higher energies, in the nuclear fusion concept, the solution (15)-(18) is considered as a relaxed minimum energy state of a plasma in a spheromak device (i.e., inside a spherical shell that confines the plasma) [21, 25]. In general, the solutions of the system of equations (10), (11) and (12) are the "natural end configurations" in a magnetically dominated plasma, because the magnetic turbulence drives such plasma towards the spheromak state [24, 25]. We suggest that similar stabilized configurations may arise in the quark-gluon plasma created in heavy-ion collisions.

BASIC PHYSICAL FEATURES OF KNOTS

Phase. The interior of the knot should be in a deconfined state with unbroken chiral symmetry. The deconfinement is needed for the quarks to flow freely inside the knot, so that they should be able to produce stabilizing magnetic fields. The chirally restored symmetry is also very important because in this state the chiral condensate is zero. A presence of the chiral condensate would wash out the imbalance between the left-handed and the right-handed quarks, leading to vanishing chiral conductivity [10], $\sigma_\chi = 0$. The very existence of the knot is guaranteed by a nonvanishing value of σ_χ, and therefore the knot cannot exist if its interior is in the chirally broken phase. The chirally restored and simultaneously deconfined phase is expected to be produced at the RHIC facility and at the ALICE/LHC experiment [26], so that the knots have a chance to be created there.

Generally, one may expect that the cold exterior outside the knot should provide an additional factor that stabilizes the knot. The nonzero tension of the interface between the phases would squeeze the knot increasing the energy density of the magnetic field, and generating a backreaction force from the inside. A qualitative illustration of the knot structure is presented in Fig. 2.

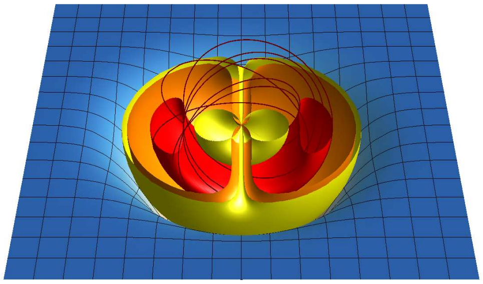

FIG. 2. A free hot knotted solution (15)–(18) in the cold QCD vacuum. The tori that host the magnetic lines of Figs. 1(a)-(c), and some of the magnetic lines are shown.

The electric charge of the knot is zero. Other important parameters of the knot may be expressed via two free parameters of the solution (15)–(18): the magnetic field scale B_0 and the chiral conductivity σ_χ.

The knot radius R_0 is given by Eq. (14).

The total magnetic energy of the knot is

$$E_{\rm magn} = \frac{1}{2} \int {\rm d}^3 r\, \vec{B}^2(\vec{r}) = C_E \frac{B_0^2}{\sigma_\chi^3} \equiv \frac{C_E}{\kappa_0^3} B_0^2 R_0^3\,, \quad (19)$$

where $C_E = (4\pi/3)\kappa_0 \sin^2 \kappa_0 = 17.9337\dots$.

The total magnetic moment of the knot is

$$\vec{M} = \int {\rm d}^3 r\, \frac{1}{2} \vec{r} \times \vec{j} = C_M \frac{B_0}{\sigma_\chi^3} \hat{z} \equiv \frac{C_M}{\kappa_0^3} B_0 R_0^3 \cdot \hat{z}\,, \quad (20)$$

where $C_M = \pi^2 [1 - (1 + \kappa_0^2/2) \cos \kappa_0] = 33.6592\dots$ and $\hat{z}$ is the unit vector along the z-axis.

The flavor content of the knot is constrained by the requirement of stability of the knot with respect to direct quark-antiquark annihilations. This implies that the interior of the knot may consist of either u, d and s quarks, *or* $\bar{u}$, $\bar{d}$ and $\bar{s}$ antiquarks. A mixed interior, say, u, d and $\bar{s}$ is less favorable energetically. The presence of heavier quarks – with the masses heavier than a few T_c – is dynamically suppressed.

The condition of the local electric neutrality [here $n_f = n_f(x)$ is the density of quarks of $f^{\rm th}$ flavor],

$$\rho = 0\,, \qquad \rho \equiv \sum_f e_f n_f = \frac{2e}{3} n_u - \frac{e}{3} n_d - \frac{e}{3} n_s\,, \quad (21)$$

sets the constraint on the total quark numbers N_f:

$$2 N_u = N_d + N_s \quad \text{with} \quad N_f = \int {\rm d}^3 r\, n_f(\vec{r})\,. \quad (22)$$

A similar relation holds for the antiquarks in a knot made of antimatter. Due to relatively large mass of the strange quark we expect that the strange fraction, $\beta_s = N_s/(N_u + N_d + N_s)$, should be low, $\beta_s \ll 1$. Thus, the flavor composition of the knot's interior should be similar to the one of a neutron star, $N_d \simeq 2 N_u$.

The minimal baryon charge of the knot,

$$Q_B = \frac{1}{3} \sum_f N_f = \frac{1}{3} (N_u + N_d + N_s)\,, \quad (23)$$

can be estimated as follows. The local electric current is

$$\begin{aligned} \vec{j}(\vec{r}) & \equiv \sum_f e_f n_f(\vec{r}) \vec{v}_f(\vec{r}) \quad (24) \\ & = \frac{2e}{3} n_u \vec{v}_u - \frac{e}{3} n_d \vec{v}_d - \frac{e}{3} n_s \vec{v}_s\,, \end{aligned}$$

where $\vec{v}_f$ is the speed of the quarks of $f^{\rm th}$ flavor. A minimal value of the baryonic charge is reached in the case of the maximal "charge-parity polarization", i.e. when all positively charged quarks (u) are, say, left-handed while the negatively-charged quarks (d and s) are all right-handed. In this case the CME-driven (2) current takes its maximum value at a fixed baryon charge. In the strong external magnetic field positively charged u quarks and negatively charged d and s quarks move in opposite directions. Ignoring a contribution of the strange quarks (i.e., setting $\beta_s = 0$), one gets $\vec{v}_u = -\vec{v}_d$ for the light quarks which travel almost with the speed of light, $|\vec{v}_{u,d}| = 1$. Using (22), we get the absolute value of the current:

$$j(\vec{r}) \equiv |\vec{j}(\vec{r})| = \frac{4e}{3} n_u(\vec{r}) = \frac{2e}{3} n_d(\vec{r})\,. \quad (25)$$

Equation (2) then allows us to express the quark's densities $n_{u,d}$ via the magnetic field of the solution (15)–(18). Then the baryon charge of the knot (23) is:

$$Q_B = \frac{3}{4e} \int {\rm d}^3 r\, j(\vec{r}) = C_Q \frac{B_0}{e \sigma_\chi^2} \equiv \frac{C_Q}{\kappa_0^2} \frac{B_0 R_0^2}{e}\,, \quad (26)$$

where $C_Q = 80.4854\dots$. The knots made of antimatter have a negative baryonic charge, $Q_B = -|Q_B|$.

In a real physical environment of heavy-ion collisions the approximate characteristics of the knot can be estimated as follows. At high temperature T the chiral conductivity is [10]:

$$\sigma_\chi = \frac{3 \overline{q^2}}{2\pi^2} \frac{|n_5|}{T^2 + \mu^2/\pi^2}\,, \qquad \overline{q^2} = \frac{1}{N_f} \sum_f e_f^2\,, \quad (27)$$

where N_f is the total number of participating quark flavors, $\overline{q^2}$ is the average squared electric charge of these flavors, μ is the quark chemical potential, and $n_5 = c_5 \cdot {\rm fm}^{-3}$ is the chiral density given by the difference between the number of left- and right-handed quarks per unit volume. Here $c_5 = 2 N_f Q_w$, where Q_w is the topological winding number (accumulated) per fm^3.

For a qualitative estimation of the knot's parameters in Pb-Pb collisions at ALICE, we take $N_f = 2$ (so that $\overline{q^2} = 5\, e^2/18$) and we assume that scale of the finite chemical potential is the same as the temperature scale, $\mu/\pi \sim T$. Thus, slightly above the phase transition, $T \sim 200\,{\rm MeV}$, one gets $\sigma_\chi \sim 0.4\, c_5\, {\rm MeV}$. Then the knot radius (14) is $R_0 \sim (2 \cdot 10^3 / c_5)\,{\rm fm}$. Typically [9, 10], $c_5 = (1 - 10)$ so that the typical radius of the knot is as small as $R \sim 200\,{\rm fm}$. This length is large compared to a geometrical scale (∼10 fm) of a typical heavy-ion collision, so that a creation of such large knot is unlikely. However, very large fluctuations of the topological charge in particular events are not excluded. Thus, in our qualitative estimation we set $Q_w \sim 50$ per fm^3, that gives us $c_5 \sim 200$ and $\sigma_\chi = 80\,{\rm MeV}$. As for the scale of the magnetic field B_0, we take a fraction of the peak value (1), $e B_0 \sim m_\pi^2$. Then we get the radius (14), the total magnetic energy (19), the total magnetic moment (20) in terms of the nuclear magneton $\mu_N = e/(2m_p)$, and the minimal baryon charge (23) of the knot, respectively:

$$\begin{array}{rclrcl} R_0 & \sim & 10\,\mathrm{fm}\,, & E_{\rm magn} & \sim & 150\,\mathrm{GeV}\,, \\ |\vec{M}| & \sim & 2.5\cdot 10^4\,\mu_N\,, & Q_B & \sim & 2.5\cdot 10^3\,. \end{array} \qquad (28)$$

The radius of the knot R_0 is of the order of the size of the lead nucleus. The magnetic energy of the knot $E_{\rm magn}$ is also a natural quantity being a bit smaller than the rest energy of the Pb nucleus. The corresponding energy density, $\varepsilon_{\rm magn} = E_{\rm magn}/(4\pi R_0^3/3) \sim 35\mathrm{MeV/fm}^3$ is much smaller than the non-equilibrium energy density regime of ALICE, $\varepsilon \simeq (1-1000)\,\mathrm{MeV/fm}^3$ [26]. The magnetic moment of the knot is rather large in nuclear units, while $|\vec{M}| \sim 15\,\mu_B$ in terms of the Bohr magneton μ_B.

The baryon charge Q_B of the knot (28) is six time larger than the total number (∼400) of nuclei in the colliding lead ions. However, the total multiplicity of produced particles in Pb-Pb collisions is estimated to be in the range of thousands [26], so that the large baryon charge Q_B of the knot may be within experimental reach.

The lifetime of the knot is difficult to estimate from general considerations since a proper analysis should involve thermal magnetodynamic calculations in a so-far-unexplored parity-odd backgrounds. We hope that this analysis can be done using a numerical approach.

GEOMETRY OF THE KNOT DECAY

The knot may be observed via the particles produced by its decay. Besides the specific flavor content (the u and d quarks should appear in proportions 1:2), the flow of produced particles is rather unusual as we will see below.

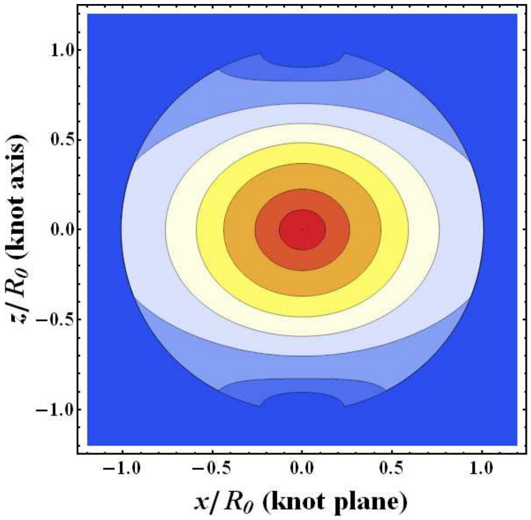

FIG. 3. The contour plot of the strength of the electric currents $\varrho = |\vec{j}(\vec{r})|/(\sigma_\chi B_0)$ in the transverse xz plane (determined by $y = 0$) of the knot. The contour lines (from outer to inner) correspond to $\varrho = 0.05, 0.1, 0.2, 0.3, 0.4, 0.5, 0.6, 0.65$.

Although the knot occupies the spherical region, the knot's interior has a lower (axial) symmetry. The spatial distribution of the magnetic energy density has a form similar to the one of an oblate (disk-shaped) spheroid. The short axis of the spheroid is parallel to the magnetic moment (20) of the knot (z-axis in our notations), while the short axes are located in the plane of the knot (xy-plane). A contour plot of the strength of the electric currents in a transverse xz plane of the knot is shown in Fig. 3. The standard eccentricity of the electric currents in the knot is negative:

$$\epsilon_j = \frac{\langle z^2 - x^2\rangle_j}{\langle z^2 + x^2\rangle_j} = -0.168\ldots\,, \qquad (29)$$

where $\langle\ldots\rangle_j = \int \mathrm{d}x\mathrm{d}z \ldots j(x,z)$. In the contrary, an initial geometry of a noncentral heavy-ion collision has an almond shape characterized by a positive eccentricity.

A decay of a knot should produce particles that dominantly follow the current distribution of the quark's current in the equilibrium state of the knot. Using the explicit knot solution (15)–(18) one can calculate the distribution of the decay products

$$\frac{\mathrm{d}^2 N}{\mathrm{d}\phi\,\mathrm{d}\varphi} = \int \mathrm{d}^3 r\,|j(\vec{r})|\delta\Big(\hat{n}(\phi,\varphi) - \hat{j}(\vec{r})\Big)\,, \qquad (30)$$

where $\hat{j}(\vec{r}) = \vec{j}(\vec{r})/|\vec{j}(\vec{r})|$ is the unit vector in the direction of the quark current at point $\vec{r}$, and $\hat{n}(\phi,\varphi)$ is the unit vector pointing in the direction determined by the polar angle φ and the new azimuthal angle $\phi = \pi/2 - \theta$. The angle ϕ gives inclination from the xy plane (we follow the standard notations used in physics of the heavy-ion collisions).

An explicit calculation reveals that the distribution (30) is independent of the polar angle φ, so that the decay of the knot is axially symmetric with respect to rotations around the z-axis. However, the azimuthal distribution of the particles emitted from the decaying knot is quite nontrivial (Fig. 4) as it differs significantly from a typical azimuthal distribution of particles produced in heavy-ion collisions.

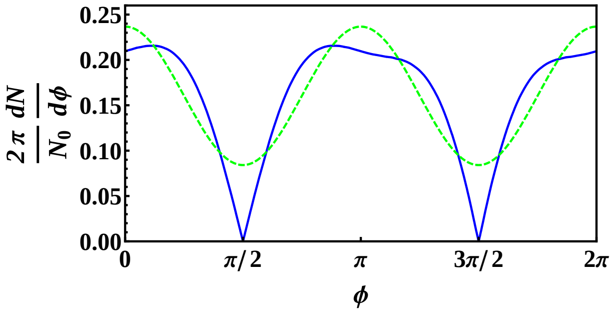

FIG. 4. Normalized azimuthal distribution of particles created in the knot decay (the solid blue line), and its elliptic component (the dashed green line).

The azimuthal particle distribution can be expanded into a Fourier series,

$$\frac{2\pi}{N_0}\frac{\mathrm{d}N}{\mathrm{d}\phi} = 1 + 2\sum_{k=1}^{\infty}\Bigl[v_k\cos(k\phi) + w_k\sin(k\phi)\Bigr]\,, \quad (31)$$

were N_0 is the total number of the particles produced in the knot decay. Symmetries of the knot imply that $v_{2k-1} = w_{2k} = 0$ with $k \in \mathbb{N}$.

The first five nonzero v- and w-coefficients of the Fourier expansion (31) are summarized in Table I. The direct flow of the knot decay is zero, $v_1 = 0$, while the elliptic flow is rather large, $v_2 \approx 1/4$. The elliptic harmonic, $1 + 2v_2\cos(2\phi)$, is shown in Fig. 4 by the dashed green line. Notice, that the higher-order v-harmonics are not small. For example, the ratio of fourth and (squared) second cosine coefficients is negative and large in its absolute value,

$$v_4/v_2^2 = -2.01\ldots\,, \quad (32)$$

contrary to the case of the heavy-ion collisions where one expects $v_4/v_2^2 \approx 0.5$ [27].

TABLE I. The Fourier flow coefficients of the particles produced in the knot decay.

n	1	2	3	4	5
v_{2n}	0.2378	-0.1138	0.04425	-0.02389	0.01505
w_{2n-1}	0.001695	0.01619	0.005640	-0.002061	0.001731

In the contrast with the heavy-ion collisions, the sine-terms of the expansion (31) are nonzero. This fact indicates that the knot decay is asymmetric with respect to the $z \to -z$ flips: the distribution of the emitted particles, say, above the xy plane does not coincide with the distribution that is observed below the plane. The z-axis asymmetry is consistent with the fact that the magnetic moment of the knot is nonzero.

The form of the azimuthal distribution, Fig. 4, signals that the largest flux of the decay products is emitted a bit above the knot's plane. The maximal flow is concentrated around the cone with the azimuthal angle

$$\phi_{\max} = 0.343\ldots \quad \text{or} \quad \phi_{\max} \approx 20^o\,. \quad (33)$$

The flow of the decay particles in the direction of the knot axis ($\phi = 0, \pi$) is zero.

Finally, we notice that it is likely that the plane of the knot may tend to coincide with the reaction plane of a noncentral heavy-ion collision that creates the knot. Indeed, the strongest magnetic field – created in the center of the collision – is perpendicular to the reaction plane while the strongest magnetic field of the knot (observed in its center, Fig. 3) is perpendicular to the knot's plane, Fig. 5. Since the knot is formed via a reconnection process of the lines of the magnetic field created in the collision, the orientations of the magnetic field lines of the collision and of the knot are likely to be correlated. This fact, in turn, implies a correlation of the corresponding planes.

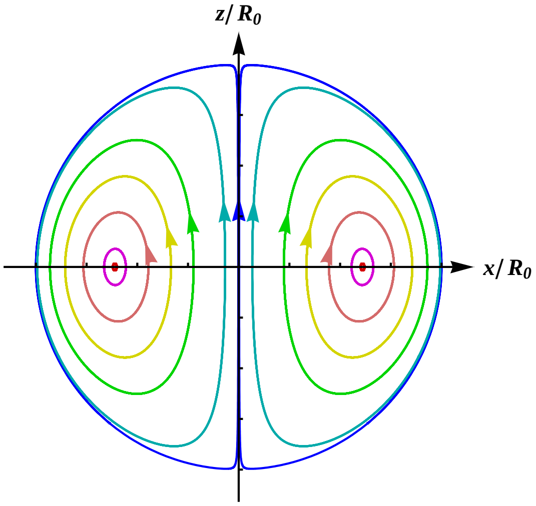

FIG. 5. The *projection* of the magnetic field lines on the $y = 0$ cross-section of the knot. The lines have, in general, a $\hat{y}$ component (not shown).

SUMMARY

In the summary, we outline our vision of the life of a typical magnetized knot.

Creation. A noncentral collision of two heavy ions creates a dense hot medium (plasma) of quarks and gluons pierced by lines of a strong magnetic field. The magnetic field – that is induced by moving charged ions and products of their collision – is perpendicular to the reaction plane. The dense quark-gluon matter expands and cools down, while (some of) the magnetic lines reconnect. Simultaneously, fluctuations of the topological charge in the plasma lead to emergence of the local parity-violating domains characterized by the imbalance between the left- and right-handed quarks. The violation of the parity symmetry in the background of the magnetic field leads to the chiral magnetic effect, and the electric current start to flow along the lines of the magnetic field.

Stabilization. If the reconnected magnetic lines happen to be knotted, then the electric current creates a self-supporting state, since the current flowing at the one segment of the knot supports the magnetic field and, consequently, the electric current at other segments. Magnetic turbulence drives the plasma towards a minimum energy configuration that resembles the Taylor spheromak state in the magnetically confined plasmas of nuclear fusion devices. Both the closeness of the knotted magnetic lines, the conservation of the electric current, and the squeezing effect of the knot boundary contribute to the stability of the knot. The magnetic lines hold the hot quark plasma confined inside the knot. The size of the knot is expected to be of the order of some tens of fermi. Generally, the knot is an electrically neutral system with a neutron-star-like flavor content: one u quark comes with two d quarks with a possible small admixture of s quarks.

Decay. As the knot cools down, the emerging chiral condensate starts to wash out the imbalance between the left- and right-handed fermions and eventually leads to the decay of the knot. We cannot estimate the lifetime of the knot using general arguments, but we expect that it should be much larger than a typical lifetime of a quark-gluon fireball created in the collision. Primary products of the knot decay are u and d quarks coming out with the specific ratio $1:2$. The emitted particles have the unusual azimuthal distribution characterized by a significant elliptic flow $v_2 \approx 1/4$, relatively large (and sometimes negative) higher harmonics (i.e., $v_4/v_2^2 \approx -2$), and axially-symmetric broad cone-shaped distribution of the emitted particles. The aperture of the emission cone is $180^o - 2\phi_{\max} \approx 140^o$. The specific flavor content and azimuthal distribution of the decay products may serve as good experimental signatures of the knots at RHIC and ALICE/LHC experiments.

The author is grateful to P. Forgacs and A.J. Niemi for useful discussions.

---

[*] On leave of absence from ITEP, Moscow, Russia.

[1] V. Skokov, A. Y. Illarionov and V. Toneev, Int. J. Mod. Phys. A **24**, 5925 (2009) [arXiv:0907.1396].

[2] E. S. Fraga and A. J. Mizher, Phys. Rev. D **78**, 025016 (2008) [arXiv:0804.1452]; Nucl. Phys. A **820**, 103C (2009) [arXiv:0810.3693].

[3] N. O. Agasian and S. M. Fedorov, Phys. Lett. B **663**, 445 (2008) [arXiv:0803.3156].

[4] I. A. Shushpanov and A. V. Smilga, Phys. Lett. B **402**, 351 (1997) [arXiv:hep-ph/9703201]; T. D. Cohen, D. A. McGady and E. S. Werbos, Phys. Rev. C **76**, 055201 (2007) [arXiv:0706.3208].

[5] V. P. Gusynin, V. A. Miransky and I. A. Shovkovy, Nucl. Phys. B **462**, 249 (1996) [arXiv:hep-ph/9509320].

[6] D. T. Son and M. A. Stephanov, Phys. Rev. D **77**, 014021 (2008) [arXiv:0710.1084].

[7] B. I. Abelev *et al.* [STAR Collaboration], Phys. Rev. Lett. **103**, 251601 (2009) [arXiv:0909.1739]; arXiv:0909.1717; see also a Viewpoint of B. Müller, Physics **2**, 104 (2009).

[8] D. Kharzeev, R. D. Pisarski and M. H. G. Tytgat, Phys. Rev. Lett. **81**, 512 (1998) [arXiv:hep-ph/9804221]; D. Kharzeev and R. D. Pisarski, Phys. Rev. D **61**, 111901 (2000) [arXiv:hep-ph/9906401].

[9] D.E. Kharzeev, L.D. McLerran, and H.J. Warringa, Nucl. Phys. A **803**, 227 (2008) [arXiv:0711.0950].

[10] K. Fukushima, D.E. Kharzeev, and H.J. Warringa, Phys. Rev. D **78**, 074033 (2008) [arXiv:0808.3382].

[11] P. V. Buividovich et al, Phys. Rev. D **80**, 054503 (2009) [arXiv:0907.0494]; M. Abramczyk, T. Blum, G. Petropoulos and R. Zhou, arXiv:0911.1348 [hep-lat].

[12] L. D. Faddeev and A. J. Niemi, Nature **387**, 58 (1997) [arXiv:hep-th/9610193].

[13] H. K. Moffatt, J. Fluid Mech. **35**, 117 (1969).

[14] M. A. Berger, Plasma Phys. Control. Fusion **41**, B167 (1999); L. D. Faddeev and A. J. Niemi, Phys. Rev. Lett. **85**, 3416 (2000) [arXiv:physics/0003083].

[15] E. Babaev, Phys. Rev. Lett. **88**, 177002 (2002) [arXiv:cond-mat/0106360].

[16] E. Radu and M. S. Volkov, Phys. Rept. **468**, 101 (2008) [arXiv:0804.1357].

[17] R. A. Battye and P. M. Sutcliffe, Phys. Rev. Lett. **81**, 4798 (1998) [arXiv:hep-th/9808129].

[18] A. F. Rañada, Lett. Math. Phys. **18**, 97(1989); W. T. M. Irvine, D. Bouwmeester, Nature Phys. **4**, 716 (2008).

[19] M. R. Dennis, R. P. King, B. Jack, K. O'Holleran, M. J. Padgett, Nature Phys., **6**, 118 (2010).

[20] S. Chandrasekhar and P.C. Kendall, Astrophys. J. **126**, 457 (1957).

[21] M. N. Rosenbluth and M. N. Bussak, Nucl. Fusion **19**, 489 (1979).

[22] J.B. Taylor, Phys. Rev. Lett. **33**, 1139 (1974).

[23] J. Cantarella, D. DeTurck, H. Gluck, M. Teyteld, Phys. Plasmas **7**, 2766 (2000).

[24] L. Woltjer, Proc. Natl. Acad. Sci. USA **44**, 489 (1958).

[25] J.B. Taylor, Rev. Mod. Phys. **58**, 741 (1986).

[26] ALICE Collaboration, J. Phys. G: Nucl. Part. Phys. **30**, 1517 (2004).

[27] C. Gombeaud and J. Y. Ollitrault, Phys. Rev. C **81**, 014901 (2010) [arXiv:0907.4664].